CHEMISTRY OF MATERIALS
Article

Chem. Mater. **2010,** *22,* 6341–6346 6341
DOI:10.1021/cm1021678

Self-Assembled Nanofilm of Monodisperse Cobalt Hydroxide Hexagonal Platelets: Topotactic Conversion into Oxide and Resistive Switching

Renzhi Ma,* Minoru Osada, Linfeng Hu, and Takayoshi Sasaki

International Center for Materials Nanoarchitectonics, National Institute for Materials Science, 1-1 Namiki, Tsukuba, Ibaraki 305-0044, Japan

Received August 1, 2010. Revised Manuscript Received September 20, 2010

The current work develops a solution-based self-assembling route to construct close-packed nanofilms (thickness ≈ 30 nm) using monodisperse hexagonal platelets of $Co(OH)_2$ as two-dimensional building blocks. The hydroxide film was postannealed and could be transformed into [111]-oriented cobalt monoxide (CoO) in a topotactic fashion retaining the original hexagonal platelet shape. Electrical resistive switching property of as-transformed CoO film was investigated, revealing a gigantic change in electrical resistance (ON/OFF current ratio: 10^3) and fast switching speed (ns level). This solution-based self-assembly procedure, in combination with a topotactic conversion from lamellar hydroxides to corresponding oxides, offers a new alternative to high-performance thin film devices based on transition metal oxide.

Introduction

Solution-based self-assembly, as a bottom-up approach that can be carried out under mild conditions, has high technical attractiveness for rational design and construction of nanoarchitectures as device components because of methodological simplicity, low cost, and low environmental impact.[1,2] Recently, monolayer films of spherical or polyhedral nanoparticles with high regularity were achieved by some solution-based techniques, e.g., Langmuir−Blodgett (LB) method[2] and oil/water interfacial self-assembly.[3,4] In contrast to nanoparticles, platelet crystallites, because of their peculiar two-dimensional (2D) anisotropy, may be naturally and easily tiled up to form a film.[5−15] Self-assembly of 2D crystallites, partly inspired by the ordered aragonite platelets in the nacreous layers of mollusk shells,[5,6] has received intensive attention for hybrid or reinforced nanocomposites, photonic and liquid crystallite applications as well as for luminescent films, etc.[9−15] In spite that it is relatively easy to align the platelets parallel to the substrate surface, in-plane azimuth orientation is usually random and the regularity is typically low,[7,14] caused by nonuniform geometric shape and broad size distribution of 2D crystallites. The cavity gaps among neighboring crystallites and low regularity hinder the uses of resulting films for high-end devices.

Layered hydroxides based on divalent transition metal ions, e.g., $Co(OH)_2$, $Co_xFe_{1-x}(OH)_2$ and $Co_xNi_{1-x}(OH)_2$, can be synthesized via homogeneous precipitation using a hydrolysis reaction.[16−19] All the hydroxide products adopt a uniform hexagonal platelet morphology with lateral size of a few micrometers (μm) whereas only tens of nanometers (nm) in thickness, offering a very high 2D anisotropy. The unique features of uniform hexagonal geometry and monodisperse size distribution promise their potential use as 2D building blocks. If these platelet crystallites can be neatly tiled into an oriented monolayer, it is highly likely to form a close-packed nanofilm with a thickness of the platelets. In particular, one intriguing property of lamellar hydroxides is that simple annealing treatment can transform them into corresponding single crystalline oxides.[20] Close-packed monolayer film of

*Corresponding author. E-mail: MA.Renzhi@nims.go.jp.

(1) Xia, Y. N.; Whitesides, G. M. *Annu. Rev. Mater. Sci.* **1998**, *28*, 153.
(2) Tao, A.; Sinsermsuksakul, P.; Yang, P. *Nat. Nanotechnol.* **2007**, *2*, 435.
(3) Mao, Z. W.; Xu, H. L.; Wang, D. Y. *Adv. Funct. Mater.* **2010**, *20*, 1053.
(4) Park, Y.-K.; Yoo, S.-H.; Park, S. *Langmuir* **2007**, *23*, 10505.
(5) Aksay, I. A.; Trau, M.; Manne, S.; Honma, I.; Yao, N.; Zhou, L.; Fenter, P.; Eisenberger, P. M.; Gruner, S. M. *Science* **1996**, *273*, 892.
(6) Smith, B. L.; Schäffer, T. E.; Viani, M.; Thompson, J. B.; Frederick, N. A.; Kindt, J.; Belcher, A.; Stucky, G. D.; Morse, D. E.; Hansma, P. K. *Nature* **1999**, *399*, 761.
(7) Lee, J. H.; Rhee, S. W.; Jung, D. Y. *Chem. Commun.* **2003**, 2740.
(8) Lee, J. H.; Rhee, S. W.; Jung, D. Y. *Chem. Mater.* **2006**, *18*, 4740.
(9) Podsiadlo, P.; Kaushik, A. K.; Arruda, E. M.; Waas, A. M.; Shim, B. S.; Xu, J. D.; Nandivada, H.; Pumplin, B. G.; Lahann, J.; Ramamoorthy, A.; Kotov, N. A. *Science* **2007**, *318*, 80.
(10) Bonderer, L. J.; Studart, A. R.; Gauckler, L. J. *Science* **2008**, *319*, 1069.
(11) van der Kooij, F. M.; Kassapidou, K.; Lekkerkerker, H. N. W. *Nature* **2000**, *406*, 868.
(12) van der Beek, D.; Radstake, P. B.; Petukhov, A. V.; Lekkerkerker, H. N. W. *Langmuir* **2007**, *23*, 11343.
(13) Lin, T.-H.; Huang, W.-H.; Jun, I.-K.; Jiang, P. *Chem. Mater.* **2009**, *21*, 2039.
(14) Hu, L.; Ma, R.; Ozawa, T. C.; Geng, F.; Iyi, N.; Sasaki, T. *Chem. Commun.* **2008**, 4897.
(15) Hu, L.; Ma, R.; Ozawa, T. C.; Sasaki, T. *Angew. Chem., Int. Ed.* **2009**, *48*, 3846.
(16) Liu, Z.; Ma, R.; Osada, M.; Takada, K.; Sasaki, T. *J. Am. Chem. Soc.* **2005**, *127*, 13869.
(17) Ma, R.; Liu, Z.; Takada, K.; Iyi, N.; Bando, Y.; Sasaki, T. *J. Am. Chem. Soc.* **2007**, *129*, 5257.
(18) Ma, R.; Takada, K.; Fukuda, K.; Iyi, N.; Bando, Y.; Sasaki, T. *Angew. Chem., Int. Ed.* **2008**, *47*, 86.
(19) Liang, J.; Ma, R.; Iyi, N.; Ebina, Y.; Takada, K.; Sasaki, T. *Chem. Mater.* **2010**, *22*, 371.
(20) Kobayashi, Y.; Ke, X.; Hata, H.; Schiffer, P.; Mallouk, T. E. *Chem. Mater.* **2008**, *20*, 2374.

Published on Web 11/16/2010

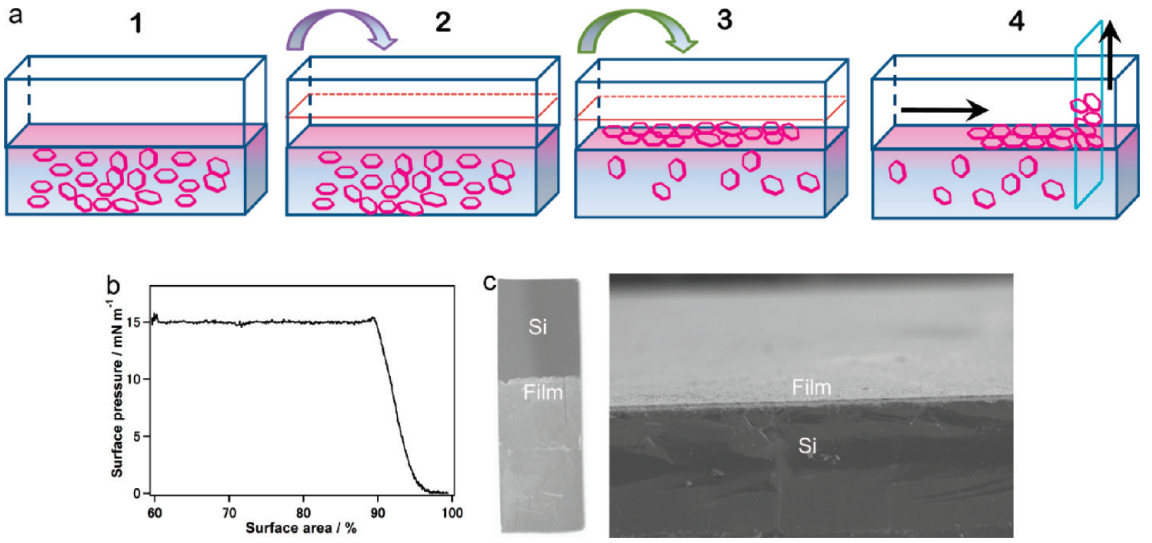

Figure 1. (a) Schematic illustration of hexane/water interfacial self-assembling procedure. Step 1: Preparing an aqueous suspension of hexagonal platelet crystallites in a Langmuir trough. Step 2: Adding hexane to form a hexane/suspension interface. Step 3: Injecting alcohol to trap the platelet crystallites to the hexane/suspension interface, forming a monolayer film. Step 4: After hexane is evaporated or extracted, the monolayer film can be transferred to a substrate in vertical lifting method. (b) Pressure−area (π−A) curve for the film transfer under a constant surface compression pressure of 15 mN m^{-1}. For the abscissa axis, the percentage of surface relative to the area before compression and film transfer is used. (c) Photograph (left panel) and cross-section SEM image (right) of continuous monolayer film deposited on Si substrate.

transition metal oxides with a thickness tens of nm is thus expected to be obtained.

Electrical resistive switching device is being studied as a promising candidate for next-generation nonvolatile memory.[21,22] Various binary transition metal oxides (e.g., CoO, NiO, TiO_2) were reported to exhibit giant changes in electrical resistance and compatible with current CMOS technology.[21−26] The device is typically based on a thin film of oxide semiconductor or insulator, in which conduction in the thickness direction can be switched on or off by external electric field. This requires a nanoscale film thickness (tens of nm to a few hundred nm) and highly dense coverage (to eliminate leak currents). Recently, typical switching characteristics were also confirmed in a NiO nanocapacitor array with a diameter of about 30 nm and a thickness of about 33 nm.[26] Up to date, all the oxide nanofilms and nanocapacitor array were fabricated in sophisticated physical deposition systems represented by pulsed laser deposition or magnetron sputtering. High-quality transition metal oxide films, self-assembled and converted from aforementioned monolayer layered hydroxide crystallites, are regarded desirable for electrical resistive switching device application because of the ideal film thickness (tens of nm), close-packed coverage, and single crystallinity, as well as the expectation to dramatically reduce manufacturing costs.

(21) Waser, R.; Aono, M. *Nat. Mater.* **2007**, *6*, 833.
(22) Seo, S.; Lee, M. J.; Seo, D. H.; Jeoung, E. J.; Suh, D.-S.; Joung, Y. S.; Yoo, I. K.; Hwang, I. R.; Kim, S. H.; Byun, I. S.; Kim, J.-S.; Choi, J. S.; Park, B. H. *Appl. Phys. Lett.* **2004**, *85*, 5655.
(23) Shima, H.; Takano, F.; Tamai, Y.; Akinaga, H.; Inoue, I. H. *Jpn. J. Appl. Phys.* **2007**, *46*, L57.
(24) Shima, H.; Takano, F.; Muramatsu, H.; Yamazaki, M.; Akinaga, H.; Tamai, Y.; Inoue, I. H.; Takagi, H. *Appl. Phys. Lett.* **2008**, *93*, 113504.
(25) Kwon, D.-H.; Kim, K. M.; Jang, J. H.; Jeon, J. M.; Lee, M. H.; Kim, G. H.; Li, X.-S.; Park, G.-S.; Lee, B.; Han, S.; Kim, M.; Hwang, C. S. *Nat. Nanotechnol.* **2010**, *5*, 148.
(26) Son, J. Y.; Shin, Y.-H.; Kim, H.; Jang, H. M. *ACS Nano* **2010**, *4*, 2655.

In the present work, monodisperse hexagonal platelets of $Co(OH)_2$ are successfully close-packed into a monolayer film (~30 nm) through an oil/water interfacial self-assembly procedure. The hydroxide film is postannealed and converted into CoO in a topotactic fashion, which exhibits high potential to be used as electrical resistive switching device.

Experimental Section

Synthesis. Hexagonal platelets of $Co(OH)_2$ were synthesized from a previously reported homogeneous precipitation method using a dilute aqueous solution of $CoCl_2 \cdot 6H_2O$ refluxed with HMT.[16] The crystallites exhibit average lateral size (length of one side) of several μm but a thickness of ~30 nm, i.e., a very high aspect ratio >100 (see Figure S1 in the Supporting Information). Reaction parameters such as initial metal ion concentration, amount of HMT, reaction temperature and time were optimized to establish right conditions for the synthesis of monodisperse crystallites. Two typical types of platelet with different average lateral size, ~4 μm and ~2 μm, were synthesized from initial $CoCl_2 \cdot 6H_2O$ concentrations of 5 mM and 7.5 mM, respectively. After synthesis, gravitational sedimentation and centrifugation (500 rpm, 10 min) were performed repeatedly (7−10 times) to further improve the size monodispersity.

Film Fabrication and Transformation. Silicon (100) wafer and quartz glass substrate were cleaned by immersing in 1:1 HCl/CH_3OH solution and then in concentrated H_2SO_4 for 30 min each, while conductive Pt substrate, Pt deposited on the thermally oxidized Si substrate with an adhesion Ti layer, was photochemically cleaned by irradiation under UV light in ozone atmosphere.

An oil/water interfacial self-assembling procedure was employed to fabricate a monolayer film of $Co(OH)_2$ platelet crystallites.[3,14] A schematic illustration of the procedure is shown in Figure 1. $Co(OH)_2$ pink crystallites (80 mg) were first dispersed in 80 cm^3 Milli-Q water and poured into a Filgen LB40-KBC Langmuir trough (Teflon coating, active trough surface area 24.3 × 5 cm^2, trough volume 100 cm^3) equipped with a Wilhelmy balance for

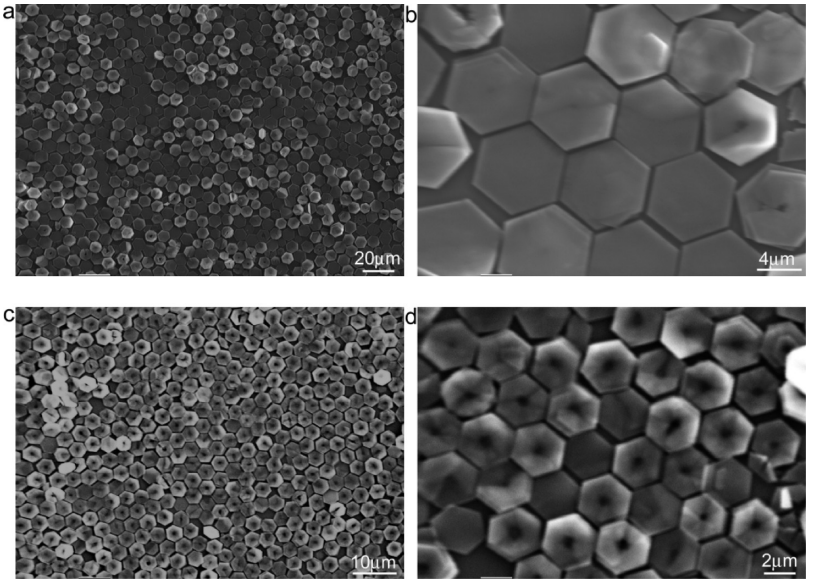

Figure 2. SEM images of monolayer films using $Co(OH)_2$ platelet crystallites of different lateral sizes: (a, b) ~4 and (c, d) ~2 μm.

surface pressure measurement. Hexane (8 cm^3) was then added to form a hexane/water interface. Butanol (1.5 cm^3) was slowly injected to the interface at a rate of 0.1 cm^3 min^{-1} using a Hamilton syringe operated by Harvard Apparatus syringe pump (MA1 70−228). Pink $Co(OH)_2$ crystallites were observed to swarm to the hexane/water interface immediately from the aqueous subphase, forming a visible continuous film. After most of hexane was evaporated, the film at the interface was then compressed at 3 mm min^{-1} until a surface pressure of 15 mN m^{-1} was reached (Figure 1b). It was then transferred onto a solid substrate using the vertical lifting method at a transfer rate of 3 mm min^{-1} while maintaining a constant pressure 15 mN m^{-1}. By this procedure, a continuous film can be obtained on different substrates such as Si wafer (Figure 1c), quartz glass, and Pt substrate.

Fabricated $Co(OH)_2$ films were either heated at 600 °C for 10 min in a vacuum by an infrared image furnace (MILA-3000) or at 800 °C for 2 h in air by a Muffle furnace to be converted into CoO or Co_3O_4, respectively. For as-converted CoO films on conductive Pt substrate (bottom electrode, BE), Ta or Pt metals were also deposited using a shadow mask to act as top electrodes (TE).

Sample Characterization. X-ray diffraction (XRD) data were recorded by a Rigaku RINT-2200 diffractometer with monochromatic Cu K_α radiation (λ = 0.15405 nm). Morphology of the synthesized products and monolayer films was examined using a Keyence VE8800 scanning electron microscope (SEM). Transmission electron microscopy (TEM) characterization was performed on a JEOL JEM-3100F transmission microscope. UV−vis absorption spectra were recorded using a Hitachi U-4100 spectrometer. Hard X-ray photoelectron spectroscopy (HX-PES) was performed at SPring-8 (BL15XU, hν = 5.95 keV at 300 K). Binding energy was calibrated using the Fermi level of gold film. Electric measurements were carried out on a Keithley 4200-SCS semiconductor parameter analyzer equipped with pulse generator. Measurements on individual platelet crystallites were performed with a conducting Pt/Ir-coated Si cantilever by an SII Nanotechnology E-Sweep atomic force microscope (AFM).

Results and Discussion

During interfacial self-assembling procedure, $Co(OH)_2$ crystallites suspending in aqueous subphase in a Langmuir trough has a contact angle $< 90°$ at hexane/water interface. Addition of butanol causes the change in surface energy to make it approaching 90°. As a result, the platelet crystallites are entrapped to the interface forming an oriented monolayer, which can be transferred to various substrates using vertical lifting method. Figure 2 displays typical top-view SEM images of as-fabricated films using $Co(OH)_2$ crystallites with different monodisperse sizes under a surface compression pressure of 15 mN m^{-1}. A monolayer nature is evident in these images. Hexagonal platelets are aligned parallel to the substrate surface and neatly tiled with their edges in contact basically side-by-side, forming a close-packed film on a large area. Local ordering into a hexagonal packing pattern is also apparent and more obvious in the film fabricated by using crystallites of ~2 μm lateral size than that of ~4 μm ones.

Typical XRD pattern of the film on Si (100) wafer is shown as the bottom trace in Figure 3a. Besides a peak derived from underlying Si substrate, only basal reflection series 00l (l = 1, 2, 3), indexable to brucite $Co(OH)_2$ (JCPDS74−1057) with an interlayer spacing 4.6 Å, were observed. Different from the XRD pattern on powder sample (see the Supporting Information, Figure S1c), in-plane reflections such as 100 and 110 were not observed. In brucite hydroxide, octahedral units, consisting of Co ions coordinated by six hydroxyl groups, share edges to form infinite charge-neutral layers. The XRD result thus indicates the formation of a highly oriented film along [001] direction (the layer stacking direction) of $Co(OH)_2$ platelets. In fact, this [001] orientation was also observed for $Co(OH)_2$ films fabricated on other substrates such as quartz glass and Pt (see the Supporting Information, Figure S2).

After infrared heat treatment was carried out on the hydroxide film at 600 °C for 10 min in vacuum, only two peaks, which can be indexed to 111 and 222 reflections of rocksalt cobalt monoxide (CoO, JCPDS75−0418), are identified (top trace in Figure 3a). This result indicates

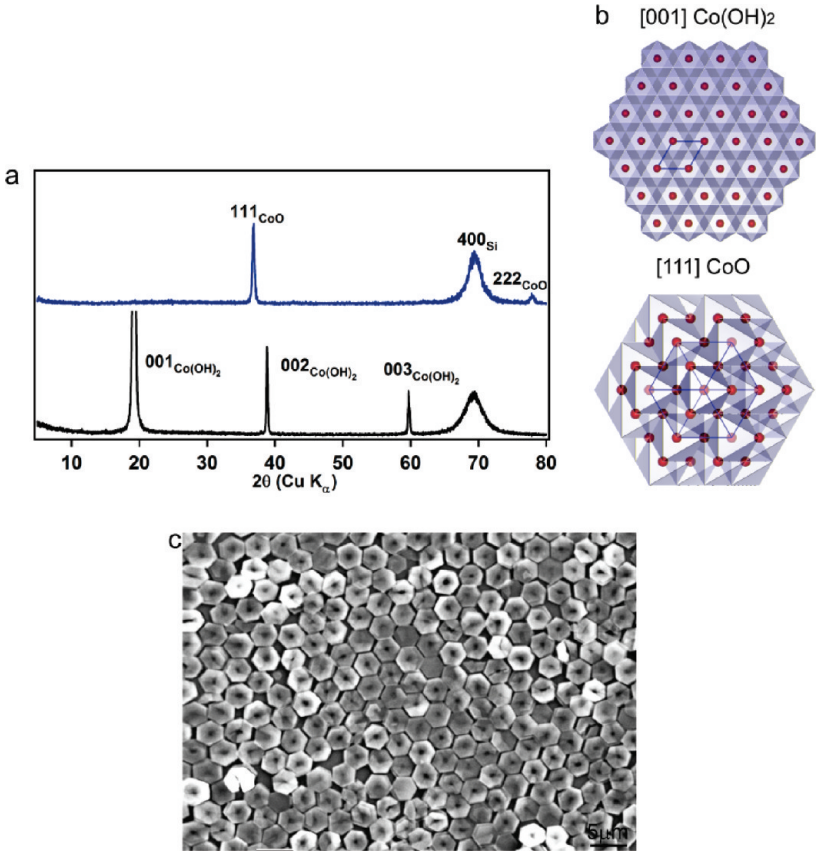

Figure 3. (a) XRD patterns of monolayer films on Si substrate before and after heat treatment in vacuum, showing [001] orientation for $Co(OH)_2$ (bottom trace) and [111] orientation for as-converted CoO (top trace), respectively. (b) Octahedral unit arrangement (center Co atoms are also shown) for $Co(OH)_2$ and CoO viewed along [001] and [111] directions, respectively. Blue lines outline unit cells. (c) SEM image of as-converted CoO monolayer film.

that the converted cobalt monoxide film is oriented along [111] direction. In the dehydroxylation process from $Co(OH)_2$ to CoO, each Co ion is still surrounded by six oxygen atoms located at the vertices of a regular octahedron. As illustrated in Figure 3b, the arrangement and coordination of metal atoms viewed along [111] in cobalt monoxide remarkably resemble to those of layered $Co(OH)_2$ along [001] direction. In other words, the chemical bonding state and coordination similar to oxides already exist in starting lamellar hydroxides. As a direct consequence, the conversion seems to be topotactic, i.e., the morphology of lamellar hydroxide crystallites is well-preserved.[20] Accordingly, a close-packed nanofilm of CoO hexagonal platelets was obtained, in which the morphological features as well as the regular ordering of $Co(OH)_2$ crystallites were exactly retained (Figure 3c). TEM characterization in Figure 4 also clearly displays that the hexagonal shape is maintained. Electron diffraction on as-transformed CoO platelets confirm that they are single-crystalline, with a vertical [111] zone axis, consistent with XRD characterizations.

Figure 5a shows UV−vis absorption spectrum of as-converted CoO nanofilm. Accordingly, the band gap E_g may be calculated from the following equation:

$$\alpha h\nu = A(h\nu - E_g)^n$$

where α is the absorption coefficient, $h\nu$ is the photon energy, A is a constant characteristic to the material, and

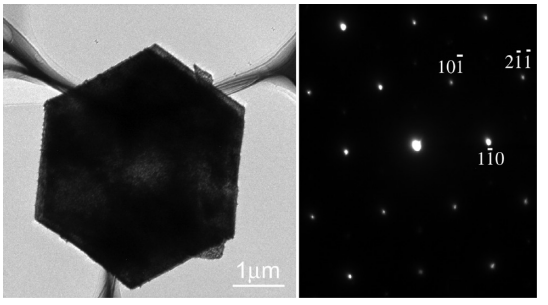

Figure 4. TEM image and electron diffraction pattern along [111] zone axis of as-converted CoO, exhibiting the topotactic feature with starting $Co(OH)_2$ crystallites.

$n = 2$ for an indirect transition or 1/2 for an allowed direct transition. By plotting $(\alpha h\nu)^{1/n}$ against $h\nu$ in eV, a straight line segment is obtained. The best fit of the equation gives $n = 1/2$ as shown in Figure 5b. The extrapolation of the straight line segment to $(\alpha h\nu)^2 = 0$ yields the absorption band gap energy of ~2.6 eV, which agrees well with the value of ~2.5 ± 0.3 eV reported for CoO as a Mott-type insulator.[27,28]

On the other hand, heat treatment in air seems to convert the $Co(OH)_2$ film into spinel Co_3O_4 (JCPDS74−2120). As-transformed Co_3O_4 is also oriented in [111] direction (see the

(27) van Elp, J.; Wieland, J. L.; Eskes, H.; Kuiper, P.; Sawatzky, G. A.; de Groot, F. M. F.; Turner, T. S. *Phys. Rev. B* **1991**, *44*, 6090.
(28) Hugel, J.; Kamal, M. *Solid State Commun.* **1996**, *100*, 457.

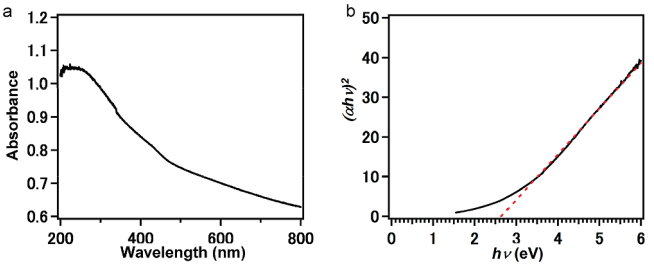

Figure 5. (a) UV−vis absorption spectrum of as-converted CoO nanofilm on quartz glass substrate. (b) Optical band gap energy of CoO obtained by extrapolation to $(\alpha h\nu)^2 = 0$.

Supporting Information, Figure S3a). However, unlike the dehydroxylation into CoO where Co^{2+} remains at octahedral sites, the formation of Co_3O_4 ($Co^{2+}Co^{3+}{}_2O_4$) requires partial oxidation of Co^{2+} (see the Supporting Information, Figure S3b) where half of the octahedral sites are populated with Co^{3+} and one-eighth of the tetrahedral sites are populated with Co^{2+} (Figure S3c). Because of such chemical and crystallographic reorganization, the phase conversion in air brings about a rough and porous surface, even some cracks, to original $Co(OH)_2$ platelets, despite that a basic hexagonal framework shape is still maintained (see Figure S3d,e in the Supporting Information). The morphological defects in Co_3O_4 are not suitable in the context of electric property measurement. In addition, Co_3O_4 is a p-type semiconductor with a lower room temperature resistivity, $\sim 1 \times 10^6$ Ω cm, than that of insulating CoO ($\sim 10^9$ Ω cm).[29,30] Therefore, as-transformed close-packed CoO nanofilm is selected for subsequent resistive switching property measurements.

Figure 6a shows an AFM image of as-converted CoO hexagonal platelets on Pt substrate. Electric resistance state of individual CoO crystallite was probed using a conducting cantilever by dc voltage sweep measurements. Typical current−voltage ($I-V$) profiles are plotted in Figure 6b. The CoO crystallite exhibited a very high initial resistance with a negligible current in pA order, which accords with highly insulating nature of Mott-type CoO.[29,30] When the voltage was increased to ~3.0 V, a sudden increase in current to 100 nA (the compliance current) was observed, indicating the change from high resistance state (HRS) to low resistance state (LRS). The LRS can also be identified by sweeping the voltage to less than 1.0 V, which reached the compliance current instantly, verifying a nonvolatile nature. When the voltage polarity was reversed and swept to −3.0 V, the LRS was destroyed at −2.8 V, restoring to initial HRS. As shown by the green profile, another voltage sweep to ~3.0 V could activate the conductive path again to attain LRS. The measurement, clearly revealing a transition between HRS (i.e., OFF) and LRS (ON) induced by external electric field, indicates that a single crystalline CoO platelet may function as a nonvolatile resistive switching memory cell.

After depositing metallic top electrodes ($\Phi = 100\,\mu$m), seen as brighter contrast discs in Figure 7a, resistive

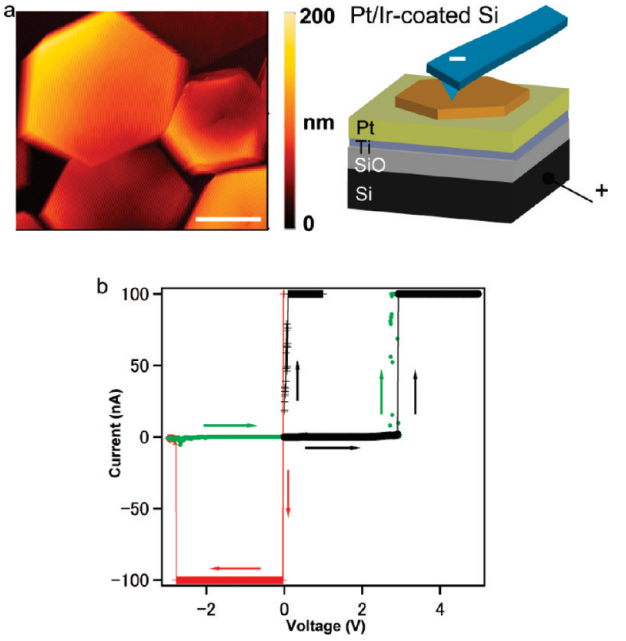

Figure 6. (a) AFM image of hexagonal platelets and schematic configuration for measuring electric resistance state on individual CoO platelets. Scale bar shown in AFM image is 2 μm. (b) $I-V$ curves by sweeping the voltage in the directions indicated by arrows. A compliance current of 100 nA is applied.

switching property of close-packed CoO nanofilm was investigated using W probe (Figure 7b). Typical current−voltage characteristics are shown in Figure 7c. Similar to individual platelet crystallites, the nanofilm also exhibited a typically high resistance $> 1 \times 10^{12}$ Ω. When the voltage was increased to ~4.5 V, an abrupt change in resistance from the high resistance state to a low resistance state of $\sim 1 \times 10^7$ Ω was observed, namely, a so-called forming process. Subsequently, a reset process, which oppositely turns LRS back to HRS, could be seen when sweeping the voltage from zero to 1.0 V. Furthermore, another voltage sweep from zero to about ~2.0 V again switched the HRS into LRS, which is considered as a set process. Fluctuation of resistance in both the HRS and LRS regimes were observed. However, a window defined by the change in two resistance states, i.e., R_{HRS}/R_{LRS}, is typically $\sim 1 \times 10^3$, which is comparable to reported values of CoO films under physical deposition.[23] The high R_{HRS}/R_{LRS} margin makes it very easy to distinguish the storage information ("1" or "0") if the nanofilm is used for the purpose of memory device. As each electrode area may cover hundreds of CoO crystallites, this result displays that the film does not have apparent leak paths, which may be accounted for by the close-packed arrangement of individual crystallites. It is also noteworthy that the reset current is very low (< 1 mA), which may make the switching speed of the reset process fast and is very beneficial for practical uses. The operating mechanism behind the resistive switching phenomenon in current CoO nanofilm is assumed similar to conventional binary oxides,[21,25] in which local conducting filament paths in insulating oxide matrix are formed during an electroforming process (forming) or Joule heating-assisted reduction (set), whereas these conducing filaments

(29) Koumoto, K.; Yanagida, H. *Jpn. J. Appl. Phys.* **1981**, *20*, 445.
(30) Borchardt, G.; Kowalski, K.; Nowotny, J.; Rekas, M.; Weppner, W. *J. Eur. Ceram. Soc.* **1994**, *14*, 369.

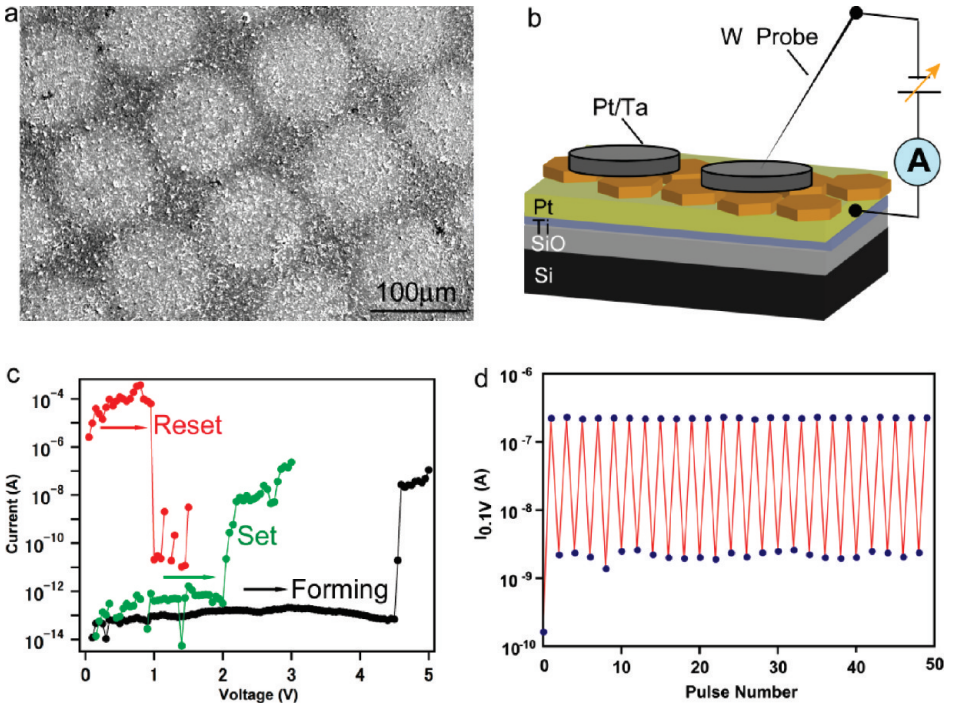

Figure 7. (a) SEM image of Pt top electrodes (diameter: 100 μm) deposited on as-transformed CoO film. (b) Schematic illustration of the resistive switching measurements. (c) $I-V$ characteristics of CoO film in semilogarithmic scale. Arrows indicate the direction of the voltage sweep. (d) Set/reset cycles stimulated by short pulses. By applying 2.8 V/20 ns pulse for set and −3.0 V/20 ns pulse for reset, respectively, the nanofilm device is reproducibly switched between HRS and LRS.

and paths are subsequently ruptured/fused as a result of Joule heating and the electric field (reset).

Figure 7d depicts a sequence of set/reset (write/erase) cycles on the CoO nanofilm stimulated by nanosecond (ns) pulses, 2.8 V/20 ns bias for set and −3.0 V/20 ns bias for reset, respectively. A small voltage of 0.1 V was used to read out the resistance states in the intervals of neighboring pulses. The stable switching between the LRS and the HRS can be seen up to 50 test runs. It highlights the presence of nonvolatile bipolar resistive switching effect in the present CoO nanofilms and the low power consumption properties.

Conclusions

Monodisperse hexagonal platelets of $Co(OH)_2$ were prepared and successfully self-assembled into an oriented and close-packed monolayer film. After being converted into CoO in a topotactic process, a gigantic change in resistance induced by external electric field has been observed. At the same time, a very fast switching between the high resistance state (OFF) and low resistance state (ON) in ns level has also been realized. Different from widely used physical deposition techniques, the present approach is based on a solution-based interfacial self-assembly in combination with the unique conversion from layered hydroxide to corresponding oxide, which is innovative in the creation of single crystalline transition metal oxide nanofilms with a thickness tens of nm, and has an advantage of low manufacturing cost and low environmental impact, even compatible with current CMOS technology. In the same manner, oxide nanofilms with different compositions are expected to be converted if other transition metal layered hydroxide platelet crystallites (e.g., $Co_xNi_{1-x}(OH)_2$ and $Co_xFe_{1-x}(OH)_2$, etc) are similarly employed. Therefore, the proposed approach may also be able to achieve precise control over composition, structure, and crystallinity of various transition metal oxide nanofilms, which is very helpful to understand electronic and magnetic properties, including resistive switching phenomenon, in association with particular crystal structure and electronic states.

Acknowledgment. This work is partly supported by World Premier International Research Center (WPI) Initiative on Materials Nanoarchitectonics, MEXT, Japan and CREST of the Japan Science and Technology Agency (JST).

Supporting Information Available: Experimental data on synthesis and characterization of starting $Co(OH)_2$ crystallites, XRD patterns of $Co(OH)_2$ films on different substrates, characterization of as-converted Co_3O_4 (PDF). This material is available free of charge via the Internet at http://pubs.acs.org.